# Detecting Tar Contaminated Samples in Road-rubble using Hyperspectral Imaging and Texture Analysis

Paul Bäcker[1], Georg Maier[1], Robin Gruna[1], Thomas Längle[1], and Jürgen Beyerer[1,2]

[1] Fraunhofer Institute of Optronics, System Technologies and Image Exploitation IOSB, Fraunhoferstraße 1, 76131 Karlsruhe, Germany

[2] Vision and Fusion Laboratory (IES), Karlsruhe Institute of Technology (KIT), Haid-und-Neu-Str. 7, 76131 Karlsruhe, Germany

**Abstract** Polycyclic aromatic hydrocarbons (PAH) containing tar-mixtures pose a challenge for recycling road rubble, as the tar containing elements have to be extracted and decontaminated for recycling. In this preliminary study, tar, bitumen and minerals are discriminated using a combination of color (RGB) and Hyperspectral Short Wave Infrared (SWIR) cameras. Further, the use of an autoencoder for detecting minerals embedded inside tar- and bitumen mixtures is proposed. Features are extracted from the spectra of the SWIR camera and the texture of the RGB images. For classification, linear discriminant analysis combined with a k-nearest neighbor classification is used. First results show a reliable detection of minerals and positive signs for separability of tar and bitumen. This work is a foundation for developing a sensor-based sorting system for physical separation of tar contaminated samples in road rubble.

**Keywords** Hyperspectral Imaging, Autoencoder, Polycyclic Aromatic Hydrocarbons

## 1 Introduction

Until the 1980s, tar was primarily used as a binder for road surface construction in Germany [1]. It has since been outlawed for the construc-

tion of new roads due to its high levels of Polycyclic Aromatic Hydrocarbons (PAHs) that have been identified to be carcinogenic, mutagenic and genotoxic and can contaminate the groundwater [2]. Further, the use of recycled tar containing materials as a foundation of new road surfaces has been restricted.

Other materials present in road rubble are bitumen, which replaced tar as binder material, and minerals, which make up the biggest part of the road surface mixture ($\sim$95 wt%) and are used in the road foundation. Both of these materials are valuable for recycling, but are frequently lost as they cannot be separated from the tar containing fractions. Therefore, they are deposited at a landfill, which is increasingly expensive, or fed into a highly energy consuming tar decontamination process where they are damaged due to high temperatures altering the molecular structure of the minerals.

The mixing of tar contaminated road rubble with uncontaminated bitumen and minerals is due to different road layers and repaired road patches that appear in close proximity and are therefore mixed during demolition. Further, many uncontaminated mixtures are unnecessarily declared as tar containing, as this can be cheaper for the demolition crews than carrying out the mandated testing procedures. This testing includes taking point-samples in a certain raster and having them analyzed in a laboratory.

To acquire a rough estimate over possible PAH concentration, solvent-based paints can be sprayed onto the rubble. Such paints react with the PAHs creating a fluorescent effect that is visually observable. This method is however not sufficient for official classification, as this detection method is not accurate for all PAHs and cannot be used for dense classification and sorting of all material to limit paint usage.

As part of the InnoTeer project, the entire process from the creation of rubble at the construction site to transportation, separation and decontamination is reevaluated [3]. Fraunhofer IOSB is developing a method to efficiently separate the tar from the mixture of materials using visual inspection with the goal to develop a sensor-based sorting system.

### 1.1 Related Work

Methods such as gas chromatography, high-performance liquid chromatography [4] and mass spectroscopy deliver accurate estimations of

PAH content. However, these Methods offer low throughput at a high cost and require dissolving the tested materials, rendering the methods unsuitable for recycling.

Visual methods for detecting PAHs include fluorescent spectroscopy. UV-excited fluorescence of PAH molecules in the Mid Infrared spectrum is widely used in astronomy to investigate properties of astronomical objects [5]. [6]. However, the detected PAHs are in gaseous form, which alters their fluorescence compared to PAHs in solid compounds. Quazi et al. have used fluorescent spectroscopy to detect and distinguish between different kinds of PAHs in soil samples [7]. Excitation is performed in low-wavelength regions of the visual spectrum (blue to green), detection in slightly higher wavelengths (green to red). Different excitation wavelengths have shown to excite different PAHs. In addition to detection, the varying distribution patterns of different PAHs were observed with phenantrene forming spherical particles, whereas naphtalene forms a uniform film. The approach seems promising, however the analysis was carried out in microscopic scale and at low speeds (several seconds for a $200 \times 200\mu$m patch). Adaptation of this method to the macroscopic scale has to the best of our knowledge not been tried in the context of PAH detection in soil.

Li et al. use a Fourier Transform Infrared (FTIR)-Spectrometer to measure the reflectance of different PAHs in soil over a broad Mid Infrared spectrum (2500 – 16000nm) with a spectral resolution of $4\text{cm}^{-1}$ [8]. The 35 measured samples were analyzed using a hybrid variable selection approach, that combines wavelength interval selection and wavelength point selection as preprocessing for a partial least squares regression. The method shows high accuracy, but the use of a point-measuring FTIR-Spectrometer in large throughput sensor-based sorting applications is not feasible. Jahangiri et al. have investigated differences between bitumen-based asphalts in terms of different additives using a FTIR-Spectrometer [9]. This illustrates the big variety in road surfaces which further complicates the task of separating tar-from bitumen-based binder.

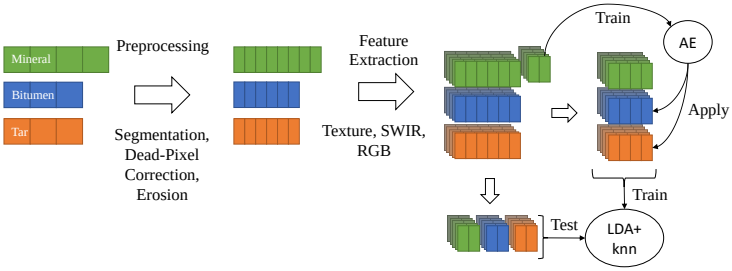


**Figure 1:** Data Processing pipeline. Preprocessing includes separating the samples from each capture and removing dead pixels. An autoencoder (AE) for detecting minerals embedded in tar and bitumen is trained on a subset of mineral features and applied to the training samples of tar and bitumen.

## 2 Materials and Methods

The problem of detecting tar in road rubble is posed as a classification problem between the classes tar, bitumen and minerals. Solving the problem requires data capture, preprocessing and classification. Preprocessing includes segmentation of the different samples, dead-pixel correction, feature extraction and a novel method for removing mineral patches embedded in the tar and bitumen samples. Figure 1 gives an overview of the different steps used in this work.

### 2.1 Samples

Samples for the classes tar and bitumen are both taken from the top layers of road surfaces and constitute a mixture of differently sized mineral elements and the binder (tar or bitumen). The class of minerals contains only solid pieces of minerals from the foundation layer. The sample size has been chosen to be between 16 and 32mm. Figure 2 shows examples of samples.

### 2.2 Data Acquisition Hardware

In this work, data from a hyperspectral Short Wave Infrared (SWIR) camera and a high-resolution RGB camera were combined for clas-

**Figure 2:** Examples for the three classes. From left to right: bitumen, tar, minerals.

sification. Both cameras are line-scanning cameras that have been mounted above the same linear stage. The linear stage carrying the samples is moving past the line-scanning cameras for image acquisition. For the hyperspectral camera, the line is illuminated using six halogen work lights. Illumination for the RGB camera is provided by two white-light LED-bars.

### 2.3 Preprocessing

As a first preprocessing step, dead-pixel correction is performed by quadratic interpolation in the spectral domain. Sample masks are automatically extracted using a binary threshold, with small artifacts being removed by morphological operation (opening) and filtering the remaining elements by size and shape.

Our goal is to be able to overlap RGB- and SWIR images (Image Registration). Therefore, the transformation between the cameras is estimated. First, the nonlinear lens distortion is calculated for each camera separately using a known calibration pattern. The resulting camera pixels are now related through a linear transformation, assuming all captured objects lie in the same plane. The main components of this transformation are a scaling factor, which is necessary because of the different resolutions and slightly different capture areas of the imaging sensors, and a translation between the cameras. These scaling and translation changes could be covered by a similarity transform (which always preserves shape). However, due to small inaccuracies in the mounting of the cameras, a more general perspective transformation is assumed (homography). The transformation matrix is estimated using a set of matching points on a calibration pattern. Using the transformation matrix, both images can be transformed into each others view.

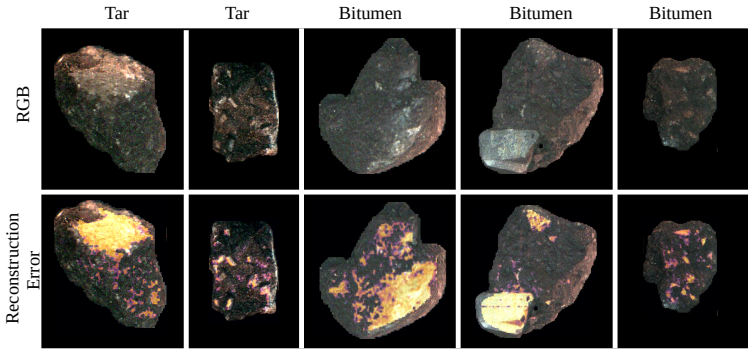


**Figure 3:** Detection of minerals in tar and bitumen. The upper row shows unedited RGB images. The lower row shows an overlay of the RGB images and a contrast-enhanced inverse reconstruction error as computed by the autoencoder.

### 2.4 Distinguishing Surface Minerals from Tar and Bitumen

A challenge when trying to distinguish between tar, bitumen and minerals is that tar and bitumen are mixtures containing large amounts of minerals (∼95 wt%) and much less solvent (∼5 wt%). Although a thin layer of binder is prevalent, there are several surface patches displaying clean minerals. Figure 3 shows examples for this.

In this work, a pixelwise autoencoder was trained on a subset of samples in the minerals-class. The in- and output of the autoencoder are spectra corresponding to a single pixel. The autoencoder is structured as a multilayer perceptron network with a latent space of 32 neurons. As a preprocessing step for tar and bitumen, the autoencoder is applied to all pixels in the training set. If the reconstructed spectrum is close to the original spectrum, it is assumed that the pixel shows a mineral (see Figure 3). These pixels are disregarded for training. This results in more homogeneous training data and increases the distance between the tar and bitumen classes and the minerals. In Section 3, the effect of this measure on classification performance is discussed.

### 2.5 Feature Extraction

In this work, classification is performed both on a pixel- and an object level. For pixelwise analysis, each pixel is initially treated as a separate sample, whereas objectwise classification uses data collected for an entire sample. As pixel features, the Standard Normal Variate-normalized spectra and their derivatives are used. Object features are the object-wide means of the spectral information as well as texture information. Since texture features require multiple pixels, they are not used in the pixelwise analysis. For texture features, the frequencies in the grayscale-converted RGB image is analyzed using Discrete Fourier Transformation and Local Binary Patterns (LBP) are extracted.

### 2.6 Classification

Classification is either performed using object features, such as extracted texture features and mean spectra, or pixelwise using only the captured spectrum of each pixel. For pixelwise classification, a majority decision (MD) is added to get the desired object wide decisions. Classification is performed using Linear Discriminant Analysis (LDA), combined with a k-nearest neighbor (KNN) classifier. The LDA reduces the feature space to $n - 1$ where $n$ is the number of different classes. Other classifiers, such as a multilayer perceptron and a support vector machine, have also been considered, but did not perform as good.

## 3 Experimental Results

Table 1 shows the recall scores for different classification methods. For all classifications, a split of 80/20 for training- and testing data was used. The classification results were cross-validated by using 50 different training/testing splits. Classification was performed either objectwise or using a pixelwise classification with a majority decision.

The pixelwise majority decision model without an autoencoder performed best with an overall recall of 93.69%. For real life scenarios, a reliable detection of tar may be more important than the maximizing recall over all classes, since small amounts of tar can suffice to render a fraction contaminated, prohibiting the use as recycled material. Therefore for the pixelwise majority decision classifiers, robust versions were

**Table 1:** Results for different classification algorithms. Values marked with an asterisk indicate that the classes bitumen and tar were treated as a single class.

| Classification Results (Recall) | | | | |
|---|---|---|---|---|
| Classifier | Features | Mineral | Bitumen | Tar |
| Objectwise | All | 96.65 | 86.86 | 83.57 |
| Objectwise M. vs. O. | Texture | 98.2 | 97.85* | 97.85* |
| Pixel MD | SWIR, RGB | 99.71 | 85.60 | 94.84 |
| Pixel MD AE | SWIR, RGB | 100.0 | 86.23 | 91.41 |
| Pixel MD robust | SWIR, RGB | 98.97 | 56.34 | 100.0 |
| Pixel MD AE robust | SWIR, RGB | 100.0 | 59.62 | 99.03 |

implemented, that assign all samples with more than 30% of pixels being classified as tar to the tar class. This achieves a perfect recall for tar samples using the pixelwise majority decision and a 99.03% recall when using the autoencoder.

The objectwise classification using both texture- and spectral features performed slightly worse overall than the pixelwise methods. However, it is more computationally which could be critical in real-world systems. For separating minerals from tar and bitumen, a single RGB camera can be sufficient to attain good separation with 98.02% of the detected minerals being true positives. This indicates the possibility of using a low-cost preselection stage using only a RGB camera to remove the minerals from the material flow.

The usage of an autoencoder for preprocessing of the training samples improves the overall classification recall for mineral and bitumen. Especially minerals can be identified consistently, as shown by the recall scores for the two models using the autoencoder. The majority decision to some degree obscures the positive effects of the autoencoder on the robustness of the detection of minerals. This improvement is observable in the overall recall over all pixels without majority decision, as shown in table 2 for pixelwise classification with- and without autoencoder. The False number of false positives in the mineral class has been halved using the autoencoder improving the recall from 98.0% to 99.19%. Recall scores for tar are slightly decreased both for the majority decision and recall over all pixels. One possible explanation for this might be that the tar samples contain a certain type of mineral that is not present in the bitumen samples. Masking out these minerals from

**Table 2:** Results for different classification algorithms on a per-pixel level.

| Pixelwise Classification Results (Recall) | | | | |
|---|---|---|---|---|
| Classifier | Features | Mineral | Bitumen | Tar |
| Pixelwise | SWIR, RGB | 98.05 | 62.27 | 71.82 |
| Pixelwise with AE | SWIR, RGB | 99.19 | 62.87 | 70.17 |

the training samples would therefore remove a means of detecting tar.

## 4 Conclusion and Future Work

In this work, we demonstrated that minerals, tar and bitumen can be distinguished using a combination of a hyperspectral SWIR camera and a RGB camera with overall recall scores of up to 93.69%. Using a robust majority decision, the recall for tar was further increased, resulting in mineral and bitumen fractions with high purity. The use of an autoencoder achieved mixed results, improving the detection of minerals and bitumen, but performing worse in the detection of tar. Possible reasons for this have been identified and will be investigated further.

A focus of future research is determining whether the achieved results generalize to all road rubble. Each of the used fractions in this study is taken from two different sources. Both tar- and bitumen based binders can include additives like rubber, polymer and fiber [9] to optimize for certain properties like temperature stability or noise generation. The utilized differences may be based in large parts on differences in these additives instead of strictly tar- or bitumen specific properties. Evaluation with additional test samples from multiple sources will therefore be needed to further validate the results.

The three classes used in this study do not include rocks used in the foundation layer that are in parts sprayed with a thin layer of PAH contaminated binder for adhesion with the higher road-layers. These foundation-layer rocks are challenging, as the surface contains patches of this adhesive binder as well as patches without this binder. For real-world applications, this class of samples will have to be addressed as well.

Finally, additional measurement systems like fluorescent spectroscopy and MWIR will be utilized to directly identify PAHs or other

chemical properties relating to tar or bitumen. An ideal solution to the problem will deliver estimates for the PAH concentration of each sample in addition to a classification.

## Acknowledgements

This work was supported by the Fraunhofer Internal Programs under Grant No. PREPARE 40-02829. Training samples were kindly provided by Zwisler GmbH.

## References

1. "Polycyclic aromatic hydrocarbons (PAH) [MAK Value Documentation, 2012]," in *The MAK-Collection for Occupational Health and Safety*. John Wiley & Sons, Ltd, 2013, pp. 1–216.
2. P. B. Farmer, R. Singh *et al.*, "Molecular epidemiology studies of carcinogenic environmental pollutants: Effects of polycyclic aromatic hydrocarbons (PAHs) in environmental pollution on exogenous and oxidative DNA damage," *Mutation Research/Reviews in Mutation Research*, vol. 544, no. 2, pp. 397–402, Nov. 2003.
3. "Material aus Straßen nachhaltig recyceln." [Online]. Available: https://www.umsicht-suro.fraunhofer.de/de/presse/pressemitteilungen/2022/InnoTeer.html
4. S. Kumar, S. Negi *et al.*, "Biological and analytical techniques used for detection of polyaromatic hydrocarbons," *Environmental Science and Pollution Research*, vol. 24, no. 33, pp. 25 810–25 827, Nov. 2017.
5. J. D. T. Smith, B. Draine *et al.*, "The Mid-Infrared Spectrum of Star-forming Galaxies: Global Properties of Polycyclic Aromatic Hydrocarbon Emission," *The Astrophysical Journal*, vol. 656, no. 2, p. 770, Feb. 2007.
6. S. Foschino, O. Berné, and C. Joblin, "Learning mid-ir emission spectra of polycyclic aromatic hydrocarbon populations from observations," *Astronomy & Astrophysics*, vol. 632, p. A84, 2019.
7. F. Qazi, E. Shahsavari *et al.*, "Detection and identification of polyaromatic hydrocarbons (PAHs) contamination in soil using intrinsic fluorescence," *Environmental Pollution*, vol. 272, p. 116010, Mar. 2021.

8. M. Li, Y. Feng *et al.*, "Quantitative analysis of polycyclic aromatic hydrocarbons in soil by infrared spectroscopy combined with hybrid variable selection strategy and partial least squares," *Spectrochimica Acta Part A: Molecular and Biomolecular Spectroscopy*, vol. 257, p. 119771, Aug. 2021.
9. B. Jahangiri, K. Barri *et al.*, "A molecular sensing method integrated with support vector machines to characterize asphalt mixtures," *Measurement*, vol. 179, p. 109528, Jul. 2021.